Chapter 11

In Vivo Heteronuclear Magnetic Resonance Spectroscopy

Blanca Lizarbe, Antoine Cherix, and Rolf Gruetter

Abstract

Magnetic Resonance Spectroscopy is a technique that has the capability of measuring metabolites in vivo and, in appropriate conditions, to infer its metabolic rates. The success of MRS depends a lot on its sensitivity, which limits the usage of X-nuclei MRS. However, technological developments and refinements in methods have made in vivo heteronuclear MRS possible in humans and in small animals. This chapter provides detailed descriptions of the main procedures needed to perform successful in vivo heteronuclear MRS experiments, with a particular focus on experimental setup in ^{13}C MRS experiments in rodents.

Key words Magnetic Resonance Spectroscopy, X-nuclei, Surface coil, Infusion, Tracer, ^{13}C labeled glucose, Mouse

1 Introduction

Heteronuclear Magnetic Resonance Spectroscopy (MRS) is based in the detection of nuclear magnetic resonances (NMR) from nuclei other than protons. In preclinical research, applications rely on the ability of MRS to noninvasively measure metabolites inside living organs, assessing the content of nuclei like ^{13}C, ^{15}N, ^{17}O, ^{19}F, and ^{31}P. One of the most common applications in heteronuclear MRS is in vivo ^{13}C spectroscopy, which can be used to determine rates of neurotransmission and neuroenergetics [1]. Notably, ^{17}O and ^{31}P measurements can determine cerebral metabolic rates of oxygen and ATP inside the mitochondria [2] and its usage is quite extended in preclinical MRS. Nonetheless, in vivo MRS of X-nuclei is challenging due to the low sensitivity detection of the non-proton nuclei; they have a substantially lower gyromagnetic ratio and typically lower natural abundance than the ^{1}H nucleus. Consequently, technical demands for its detection are very high, and, currently, in vivo heteronuclear MRS in humans is limited to a number of research groups in the world. In the past two decades, however, sensitivity and spectral resolution of MRS data has been enhanced by implementation of scanners with higher

María Luisa García-Martín and Pilar López-Larrubia (eds.), *Preclinical MRI: Methods and Protocols*, Methods in Molecular Biology, vol. 1718, https://doi.org/10.1007/978-1-4939-7531-0_11,

magnetic field strength, as well as improved radio-frequency coil designs, better radio-frequency pulse sequences, and more precise methods for localized shimming. Therefore, X-nuclei MRS techniques are becoming more and more accessible, and, especially in preclinical investigations, further studies have been published in the last years. Non-proton detection techniques, however, are—even in animal MRS—still hampered by lower sensitivity detection. Thus, implementation of a precise methodology is needed to guarantee accurate and reproducible results. On these grounds, the aim of this book chapter is to detail the procedures that are routinely implemented in preclinical in vivo heteronuclear MRS experiments. For the sake of completeness, protocols will be described first in a more general way—in terms of the nuclei investigated or substrate used—and, second, and more specifically, examples for ^{13}C detection after labeled glucose infusion in rodents will be given. Hence, the first part of this chapter is dedicated to give a general description of basics of heteronuclear NMR signal and hardware requirements; the second part provides a concise description of the materials used and the third part elaborates the description of the methodologies. Finally, an additional section called *Notes* includes extra information about specific methods that might, however, be of great interest for the reader.

1.1 Basics of Heteronuclear NMR Signal

Nuclear magnetic resonance spectroscopy is based, among other things, in detecting the resonances of the nuclei with non-zero spin ($I \neq 0$) after the application of a constant magnetic field and a radiofrequency pulse. The most commonly studied nuclei are ^{1}H, ^{31}P, and ^{13}C, although nuclei from isotopes of many other elements (e.g., ^{2}H, ^{6}Li, ^{10}B, ^{11}B, ^{14}N, ^{15}N, ^{17}O, ^{19}F, ^{23}Na, ^{29}Si, ^{35}Cl, ^{113}Cd, ^{129}Xe, ^{195}Pt) have been used in high-field NMR spectroscopy [3]. Overall, the frequency at which a specific nucleus resonates depends on the external magnetic field strength applied, the gyromagnetic ratio of the nucleus, and its chemical environment. Particularly, the dependence on the chemical milieu has its origin in two different phenomena: the shielding of the magnetic field by the surrounding electrons, on one hand, and the interactions between nuclei in the same molecule, on the other. Notably, interaction between nuclear spins is not limited to nuclei of the same type—the so-called *homonuclear coupling*—but also between different types—the *heteronuclear coupling*. This interaction between different nuclei results in a splitting of resonances into several smaller lines at different frequencies [3], and all atoms that have $I \neq 0$ are subjected to it accordingly to the chemical structure of the molecule. The splitting of the resonances complicates the understanding of the spectra, not only due to the incorporation of the additional lines but also for the decrease in signal intensity of the original (and not coupled) signal. In the study of ^{1}H NMR signals, heteronuclear coupling is normally neglected because, even though most protons

are bond to carbon molecules (at least in organic compounds), the natural abundance of ^{13}C is only around 1.1%, which almost eliminates the potential coupling effects. In non-proton detection MRS experiments, however, heteronuclear coupling becomes critical because the X-nuclei investigated are often bonded to the NMR-visible H atoms, making *proton decoupling* mandatory—and sometimes technically very challenging [4]—to obtain spectra with enough signal intensities.

There are two main techniques detecting non-proton nuclei by MRS: direct detection and indirect detection [4]. The principal characteristics that define—and distinguish—both methods are increased spectral dispersion of the resonances from the metabolites for the first one, and higher sensitivity for the second one. Consequently, depending on the type of study that is to be performed, one of the methods can be chosen. For MRS in small volumes, for example, indirect methods with higher sensitivity might be more appropriate. If a higher separation between resonances is required, then a direct detection approach should be chosen.

Direct detection methods measure the NMR signal of the X-nuclei. Excitation through RF pulses is performed at the frequency of the X-nuclei investigated, where the resonances are also received, and decoupling is performed in the ^{1}H channel. This has two immediate consequences: larger chemical shift dispersion (~30 ppm for ^{31}P NMR and >200 ppm for ^{13}C NMR) and substantial loss of sensitivity. Indeed, decreased sensitivity is a consequence of either the lower natural abundance (1.1% for ^{13}C) and/or low gyromagnetic ratio ($\gamma_{13C}/\gamma_{1H} = 0.251$, $\gamma_{31P}/\gamma_{1H} = 0.405$). Nevertheless, this low sensitivity can be overcome by the implementation of optimized methodologies, such as the exogenous administration of labeled precursors—mandatory for isotopes with low natural abundance—, polarization transfer techniques [5], or methods taking advantage of the Nuclear Overhauser Effect (NOE) [6]. Sensitivity enhancement by polarization transfer is achieved by transferring the nuclear spin polarization of protons to the X-nucleus through chemical bonds, while NOE transfers the polarization via cross-relaxation. Figure 1 shows a scheme of the original distortionless enhancement by polarization transfer (DEPT) sequence [5] (top), and a more developed version (bottom) implemented by Henry P.G. et al. [7]. In this scheme, localization is performed on the ^{1}H magnetization and the localized magnetization is subsequently transferred to carbon. This avoids potential chemical shift displacement errors induced by the large chemical shift displacement of metabolites in the ^{13}C spectra.

Another way to improve sensitivity in direct detection methods is to use hyperpolarization [8]. Hyperpolarized ^{13}C MRS has the potential to increase the sensitivity by several orders of magnitude by using a nonequilibrium polarization [9]. Particularly,

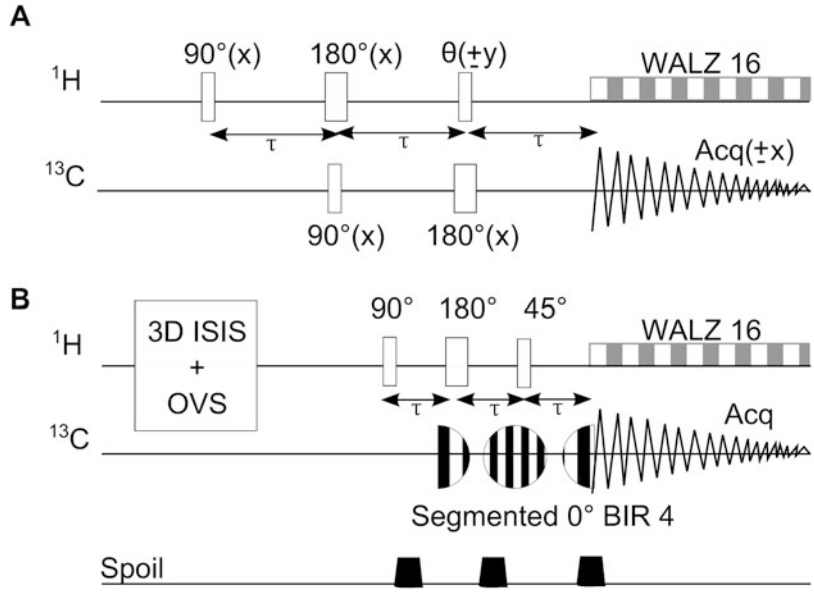

Fig. 1 ^{1}H localized broadband ^{13}C NMR spectroscopy of the rat brain in vivo at 9.4 T. (**a**) the original DEPT sequence; (**b**) modified sequence. The ^{13}C part of DEPT is replaced by a segmented adiabatic 0° BIR-4 pulse. Dephasing gradients (1 ms duration, 46 mT/m) are added between the RF pulses in DEPT to eliminate unwanted, offset-dependent coherences. The flip angle of last ^{1}H pulse is set to a nominal 45° to detect signals simultaneously from the CH, CH_2, and CH_3 groups

hyperpolarized ^{13}C MRS, due to the many technological challenges related to the generation and preservation of nonequilibrium polarization, is commonly limited to the detection of fast and dynamic metabolic pathways.

In indirect detection methods, like ^{1}H-[^{13}C], the measured signal arises from the protons that are bond to ^{13}C. In this case, the signal is transmitted and received through the ^{1}H channel and decoupling is performed at the X-nucleus frequency. The main advantage of this approach is that the larger gyromagnetic ratio of protons and its increased natural abundance leads to a significantly higher sensitivity. In fact, the sensitivity detection has been recently shown to be high enough to perform in vivo MRS experiments in the mouse brain [10], or even in small areas of it [11]. Generally, ^{1}H-[^{13}C] methods can be divided into single-shot multiple-quantum coherences-based procedures (MQC) [12] and J-difference-based methods [13]. The MQC-based methods selectively detect the ^{1}H NMR signals attached to ^{13}C nuclei by destroying, though dephasing, all other ^{1}H coherences. However, the removal of all these other ^{1}H NMR signals prevents the calculation of ^{13}C fractional enrichments (FE) and the monitoring of metabolite levels without ^{13}C label incorporation. J-difference methods, on the other hand, use the different evolution (refocusing) of the magnetization of the protons that are coupled to ^{13}C atoms, compared to

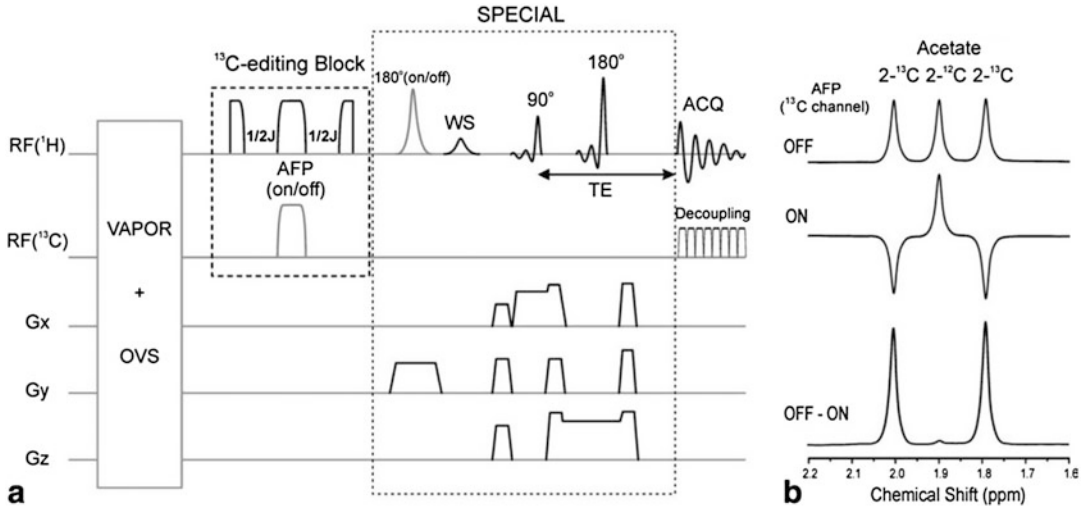

Fig. 2 (**a**) Sequence diagram of SPECIAL-BISEP (TE ¼ 2.8 ms). The editing is achieved by applying an AFP in the 13C channel on alternate scans; (**b**) in vitro validation of the editing scheme performed at 14.1 T on a solution of 67% enriched [2-^{13}C]sodium acetate (no ^{13}C decoupling during the acquisition is applied). When the ^{13}C AFP is turned off, the inversion BISEP pulse acts as a 0 BIR-4 pulse (top), while when AFP is turned on, ^{13}C-coupled ^{1}H resonances are inverted (middle). In the difference spectrum (bottom), the uncoupled resonances (^{1}H-[2-^{12}C]) are minimized and only the ^{13}C-coupled ^{1}H resonances (^{1}H-[2-^{13}C]) are detected

the refocusing magnetization of non-coupled protons, to detect both the total (^{12}C + ^{13}C) content and the ^{13}C fraction. Figure 2 depicts a scheme of the SPECIAL-BISEP sequence [14] that has been recently implemented in preclinical scanners and that allows the detection of full signal intensity ^{1}H-[^{13}C] in the mouse and rat brain.

1.2 Hardware Requirements

The performance of successful heteronuclear MRS experiments in vivo can depend on the technical requirements of the methodology. Notably, because poor sensitivity is one of the main technical issues, non-proton MRS is favored by the use of high field scanners, where the signal to noise ratio (SNR) is increased with the square root of the magnetic field B_0. Naturally, at high magnetic fields, the frequency separation between metabolites is also improved, resulting in a largely increased number of detectable metabolites at high spatial specificity. However, high fields typically are associated with increased technical challenges, such as inhomogeneous transmit (B_1) fields, an increased impact of microscopic and macroscopic susceptibility differences on static B_0 inhomogeneity, shortened T_2 and lengthened T_1 relaxation times and a lower effective B_1 field strength. Nonetheless, several studies demonstrate that the improvements achieved with the high field can largely overcome the technical challenges, extending the number of quantifiable metabolites and increasing spatial resolution and specificity [15–17]. Other limiting factors of heteronuclear MRS experiments

are the need of *designing specific RF coils,* implementation of *additional RF channels,* application of *decoupling schemes* and *adiabatic pulses.* Each of these requirements will be briefly described in the following paragraphs.

1.2.1 Design of Specific RF Coils

RF coils are frequency-dependent, and a coil that is to be used during heteronuclear NMR studies should consist of several loops, each one corresponding to the different nuclei to be investigated. Moreover, the RF coil should be designed in a way that the respective RF fields of the different loops are electrically isolated [18]. A more detailed description of the characteristics of the RF coils used in direct and indirect non-proton MRS is given in the materials section.

1.2.2 Additional RF Channels

Heteronuclear MRS experiments are only possible in spectrometers equipped with at least an additional RF broadband channel. Furthermore, acquisition has to be done in the two channels concomitantly, either during the application of decoupling schemes—proton or X-nuclei decoupling for direct or indirect detection, respectively—or during the application of inversion pulses or during polarization transfer sequences [4].

2 Materials

In the following paragraphs, a list including the main materials used during a typical in vivo MRS experiment is provided.

1. *Coil.* Standard design for RF coil for ^{13}C direct and indirect detection is generally as follows: two proton transmit/receive surface coils in quadrature lying on top of a single carbon coil [19]. However, in order to increase proton sensitivity for ^{1}H-[^{13}C] spectroscopy, an alternative has been proposed by putting the proton loops on the bottom, in order to be closer to the sample [20].
2. *External reference.* Typically, a glass sphere containing ^{13}C labeled formic acid (FA) can be at the center of the coil. This allows measuring the ^{13}C FA resonance in the magnet to set the offset for the RF pulses in the carbon channel. Furthermore, the reference allows to measure the power performance of the coil and to adjust the power for efficient 90° and 180° pulses in both proton and carbon channels. Briefly, to adjust the power values on the different channel the process is as follows: first, an experiment with a phantom is performed, and power value of a 180° hard pulse in the FA sphere is measured. Secondly, the same pulse is performed in vivo in the FA. If values in the FA change, values in the sample should change concomitantly.

3. *^{13}C labeled substrates*. Glucose is the most common substrate that allows investigating both oxidative and glycolytic metabolism; however, other substrates have been used to target specific metabolic pathways. Notably, acetate can be used to measure specifically astrocytic oxidative metabolism [21], whereas lactate can be used for investigating neuronal oxidative metabolism [22]. Besides the differences in cost, the different ^{13}C-labeled glucose substrates can be used for different purpose. It is thus primordial to choose the appropriate substrate according to the technique (mainly direct and indirect ^{13}C MRS) and the need for an increased signal relative to cost. After glycolysis, carbon positions 1 and 6 of glucose will label the methyl group of pyruvate, leading primarily to the labeling of glutamate C4 following the pyruvate dehydrogenase pathway and glutamate C2 for the pyruvate carboxylase pathway [23]. [1, 6-^{13}C] glucose is thus twice as efficient as [1-^{13}C] glucose labeling, and thus detecting, TCA cycle aminoacids. The use of [1, 6-^{13}C] glucose is particularly important for ^{13}C direct detection, in order to avoid splitting of peaks due to coupling between adjacent ^{13}C carbons. Because of this coupling, [U-^{13}C] glucose should best used in ^{1}H-[^{13}C] MRS, where decoupling in the carbon channel allows to eliminate resonances from heteronuclear coupling. [2-^{13}C] glucose can be used to investigate the anaplerotic metabolism of glial cells as it will label specifically glutamine positions C2 and C3 due to the presence of pyruvate carboxylase [24].
4. *Infusion pump*. Infusion can be done with a pump suitable for infusion from any syringe and operating in both infusion and withdrawal mode. The syringe containing the labeled glucose solution is connected to a polyethylene line that has to be long enough to cover the distance between the catheter and the pump, i.e., the distance between the animal in the magnet and the operator in the monitoring room. Adding a transparent tube connector at the end of the line can help for controlling the adjunction of the 99% enriched ^{13}C glucose bolus solution.
5. *Physiology monitoring*. Temperature of the animal can be controlled with a water circulating system covering the animal and controllable in the preparation room. Respiration and temperature can be monitored with a module located near the animal in the magnet bore and a control/gating module connected to a computer located near the operator console module. Glucose can be measured with a single drop of blood using any commercial system. Small volume sampling is critical for small animals with small blood volumes such as mice or for repeated measurements.

6. *Anesthesia*. Animal should be anesthetized in an induction chamber with 3–4% isoflurane delivered by an isoflurane vaporizer. Chamber should be connected with a gas outlet system linked to a scavenge system for isoflurane elimination. Vaporizer should be connected to both air and oxygen for a better control of animal oxygenation. The use of α-chloralose should be only limited to non-painful procedures, which require a relatively high level of brain awakeness, as this drug does not produce complete anesthesia and has poor analgesic properties. Furthermore, the only route for α-chloralose anesthesia is through intravenous (IV) administration, which can render the experiment more challenging than with isoflurane.

3 Methods

From a methodological perspective, there are two main types of heteronuclear in vivo MRS studies: experiments that require administration of exogenous tracers to increase the abundance of the isotope investigated (like ^{13}C MRS) or studies that do not need it (like in ^{31}P MRS). Naturally, studies involving infusion of labeled molecules are methodologically more complex, because they require the preparation, administration and maintenance of the solution infused. More specifically, the experimental setup for a typical ^{13}C in vivo MRS study can be divided into four main procedures, including: (1) preparation of the labeled solution, (2) animal setup, (3) MRS preparation and acquisition, and (4) administration of the labeled solution. A detailed description of each step is given in the following paragraphs. Note that for experiments not using infusion of tracers the rest of the procedures are equivalent.

3.1 Substrate Solution and Infusion Line Preparation

In vivo heteronuclear MRS experiments involve the utilization of two labeled solutions with different labeling concentration. Initially, a solution at a very high enrichment, ideally 99% enriched substrate (in labeled glucose ^{13}C MRS this means 99% content of ^{13}C and 1% content of ^{12}C in the glucose solution) is given to the animal during a short period of time. This increases rapidly the total content of labeled glucose in the animal. Secondly, a solution at a slightly lower enrichment—normally around 70%—is administered at a steady rate during the rest of the experiment. This should keep the targeted isotopic enrichment (IE) also at steady state. Remarkably, high IE's (between 50 and 100%) are convenient to allow reliable quantifications incorporated labeled carbons into glucose and its metabolites. To prepare two solutions at a different fractional enrichment, it is convenient to obtain first the 99% enriched solution and then dilute it to get the 70%. With this aim, the 99% labeled substrate should be dissolved into *phosphate-buffered saline*

(PBS) at a proportion 20% w/v. Secondly, a part of this solution can be used—we can fix 50 mL as an example—to obtain the 70% enriched one. With this aim, an additional solution of non-labeled glucose (also at 20% w/v) has to be prepared and mixed with the 50 mL of 99% enriched glucose. The specific amounts can be calculated as described in Eqs. (1)–(3).

$$50 \cdot \frac{20}{100} \cdot \frac{0.99}{1} = X \cdot \frac{20}{100} \cdot \frac{0.7}{1} \tag{1}$$

$$\Rightarrow X = \frac{9.9^{*}100}{20^{*}0.7} = 70.71\ [\mathrm{mL}] \tag{2}$$

$$\Upsilon = 70.71 - 50 = 20.71\ [\mathrm{mL}] \tag{3}$$

where X represents the mL of 70% enriched glucose and Υ the mL of non-labeled glucose. These calculations take advantage of the fact that the amount of ^{13}C glucose in the 99% enriched solution has to be the same as in the 70% enriched preparation [Eqs. 1 and (2]. In our example, this means that by adding 20.71 mL of the non-labeled glucose solution to the 50 mL 99% enriched we will obtain 70.71 mL of 70% enriched solution at 200 g/L. Note that depending on the complexity of the study two solutions might be infused at the same time. For example, during [3-^{13}C] lactate infusion studies a non-labeled solution of glucose is given concomitantly to avoid production of ^{13}C-enriched glucose from [3-^{13}C] lactate in peripheral tissues [22].

The line containing the substrate to infuse entails two separate parts; a catheter and a long polyethylene tube connecting it with the syringe containing the tracer solution. The catheter consists in a cannula that is inserted into the animals' vein plus a short plastic tubing extension, filled with PBS. The length and thickness of the line depends on the conditions of the laboratory and type of experiment performed. The line and the syringe should be filled first with the 70% enriched solution, while only a small amount of the 99% enriched substrate is used. This amount, calculated depending on the blood glucose levels and body weight (*see* Subheading 3.4), is inserted in the tip of the line and will be the first part entering the animal when infusion starts.

3.2 Animal Setup

Before putting the animal inside the scanner, the following steps should be followed:

1. *Checking general status of the animal.* Before starting an experiment, the health of the animal needs to be checked and his status reported. For ^{13}C glucose infusion experiments, the animal's body weight and blood glucose levels should be measured (*see* **Note 1**). Importantly, these values will be

needed to calculate the amount and rate of the substrate infusion (*see* Subheading 3.1).

2. *Anesthesia*. Animals can be anesthetized before insertion of the cannula(s). To sedate the animals, volatile anesthetics like isoflurane are generally used, but other sedatives might be used, depending on the type of study that is to be performed [25]. In the case of isoflurane, it should be administrated at 3–4% for induction (during approximately 3 min) and at 2% during surgery, usually within a mixture of air (70%) and oxygen (30%). If an anesthetic other than isoflurane is used—such as α-chloralose or thiopental—a second catheter in a femoral vein has to be placed for its infusion. In these cases, animals should be intubated with an endotracheal catheter and ventilated with a pressure-driven ventilator to ensure proper respiration.
3. *Insertion of the cannula*. It requires considerable expertise. To perform the femoral vein catheterization, the inguinal region of the anesthetized mouse has to be shaved. The femoral vessels should be exposed after an inguinal cut parallel to abdominal muscles. The subcutaneous branch of femoral vessels can be eventually cauterized for fewer disturbances. With help of a hemostat, the abdominal muscles must be hold above the femoral vein, pulled and put under tension. This should expose completely the femoral vein and compress it causing vasodilatation. Fibrous tissue covering the vein should be removed using blunt forceps. Catheter will be inserted 2 mm in the vein as distally as possible, while pulling the vein toward the abdomen with help of forceps in order to stretch it sufficiently. After letting go the forceps and losing tension on the hemostat, the tube of the catheter (not the needle!) has to be pushed 1 cm in the vein and the needle completely retracted. If the procedure succeeded, blood from the vein should go up in the catheter. A PBS-containing syringe is then connected to the catheter from which injection of a few microliters in the vein and withdrawal from the blood should indicate that the infusion is working. The catheter has to be fixed on the vein and leg using glue and the wound closed with silk suture. For more safety, the catheter itself should be fixed on the leg with medical tape. In experiments with rats, two catheters can be inserted: one into a femoral vein to infuse the labeled solution and a second into a femoral artery to extract blood and monitor concentration of gases, glucose, lactate, and arterial blood pressure. In studies using mice, however, because their total blood volume is small, blood extraction during infusion protocols is not routinely performed. Alternatively to femoral vein cannulation, which requires euthanasia of the animals at the end of the experiment, animals can be cannulated at the level of the lateral caudal vein (right or left). This is appropriate for

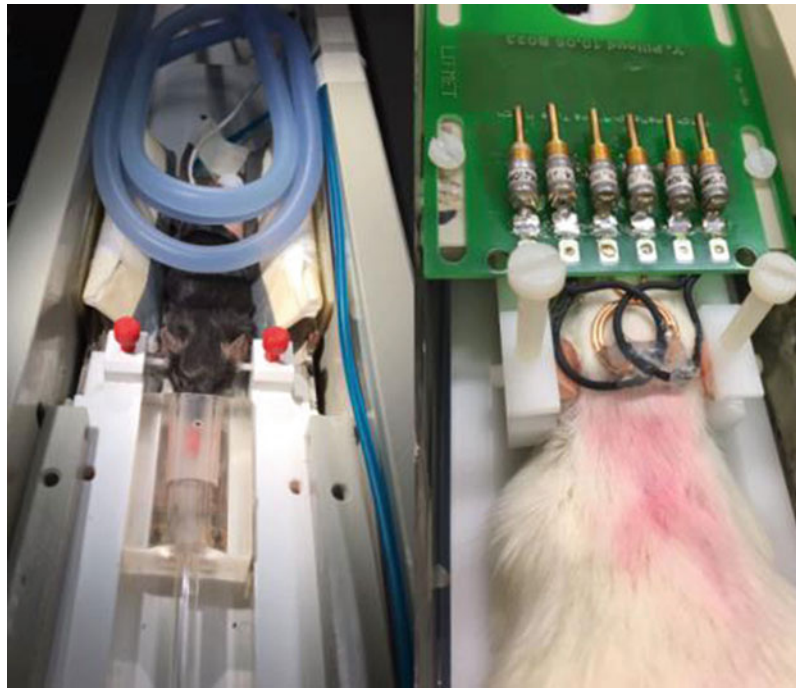

Fig. 3 Animal immobilization in holders and supporting instrumentation. Left: The mouse head is fixed through ear bars (in white) which are secured by small screwdrivers (in red). A small piece of acrylic glass covers the animal's mouth to avoid loss of anesthesia and prevent potential movements. An extra bar connects the anesthetic tubing with the animal's mouth. On the edge of this bar a small hole (in red) is used to place the animal's teeth. Blue water tubing is placed on top of the animal to maintain body temperature. The thermometer cable can be seen coming out from the mouse body. The blue tubing on the right lateral of the holder belongs to the respiration sensor, which is placed underneath of the animal's belly. Right: The rat head is fixed also through ear bars. A surface coil (double ^{1}H in quadrature and single ^{31}P) is place centered in the animals' head

longitudinal studies in which several in vivo heteronuclear MRS measurements are intended. However, tail vein cannulations are technically more challenging and several precautions need to be considered (*see* **Note 2** for extended explanation). In both cases, it is important that temperature is maintained at 37 °C during surgery.

4. *Transfer to the holder*. Pictures in Fig. 3 illustrate the elements needed to keep animals in optimal conditions during the in vivo MRS studies. Ideally, animals should be immobilized with stereotaxic fixation, to minimize potential motion during the MR session. Figure 3 shows examples of devices used to fix the rat (right) and mice (left) heads.
5. *Monitoring of the animal's physiology*. Body temperature should be monitored during all MR procedures, since anesthesia is known to decrease body temperature [25]. This is normally done using a rectal temperature probe that should be inserted

in the animals' rectum using with some vaseline. Moreover, to maintain body temperature in a physiological range—around 37 °C—, circulating water tubes can be placed covering the animal, as illustrated in Fig. 3 (left). It is also convenient to monitor breathing rhythm. In this sense, concentration of isoflurane can be adjusted in order to keep 70–100 bpm. Finally, and to avoid corneal desiccation, a protective gel can be applied on the animal's eyes.

6. *Positioning of the surface coil.* We can carefully position the surface coil into the animals' head, as shown in Fig. 3 (right) for the rat's head (*see* **Note 3** for more details) and transfer the holder into the magnet.
7. *Connecting Infusion line.* Finally, and before placing the animal in the center of the scanner, we have to arrange and connect a catheter that links the cannula in the animals' vein with the syringe containing the labeled solution.

3.3 MRS: Preparation and Acquisition

Once the animal is in the magnet, the MRS preparation before acquisition consists in: (1) positioning the holder in such a way that the area to be investigated is in the center of the magnet; (2) defining the voxel of interest (VOI), which normally involves acquisition of high resolution anatomical images, and (3) adjusting the first and second order gradient shims in the voxel [26], a process that leads to an optimized resolution of the ^{1}H spectra. Note that for defining the VOI with a good anatomical reference it might be convenient to perform T_2-weighted acquisitions. Once the VOI localization and shimming processes are performed, the type of the study and the particular conditions of the experiment will determine the type of sequences employed and the calibrations performed. A description of the potential techniques to be used and their respective adjustments is provided in the next subsections.

3.3.1 Localization Techniques

To perform single voxel MRS, approaches that limit the excitation in specific areas are used. Usually, localization is performed on the ^{1}H magnetization for both direct and indirect detection methods, but localization on the ^{13}C is frequently possible [18]. Generally, the specific conditions of the study will determine which localization method is more suitable. Single voxel MRS can be accomplished by intersecting three different RF pulses, like in Point Resolved Spectroscopy (PRESS) [27] and STimulated Echo Acquisition (STEAM) [28] methodologies. Both techniques are based on the spin echo (SE) sequence, with PRESS using a 90°–180°–180° scheme and STEAM employing three 90° pulses. In PRESS, the 90° pulse shifts the magnetization into the transverse plane, the 180° refocuses it only from one column and the last pulse refocuses magnetization in the third dimension. Since the second pulse in STEAM flips only half of the magnetization along z, only half of the

possible signal intensity is acquired. Nevertheless, the larger bandwidth of the 90° in STEAM for the same RF power implies less errors due to chemical shift displacement has and can be used with shorter echo times (TE) [29]. When short TE is used, homonuclear J-coupling evolution among protons is minimized and additional metabolites, such as glutamine, glutamate, γ-aminobutyrate, aspartate, and myo-inositol can be detected with higher signal amplitudes. Image Selected In vivo Spectroscopy (ISIS) [30] defines the VOI using an add-subtract scheme. Briefly, the localization is performed through multiple scans: in the first round of scans magnetization is flipped into the transverse plane, and in the second magnetization is inverted only in the VOI, and then flipped to the opposite side of the transverse plane. The resulting signal is subtracted, remaining only signal coming from the VOI. Since localization is achieved through multiple scans, ISIS is prone to be affected by movement, and is often employed together with other localization techniques such as Outer Volume Suppression (OVS). OVS approach defines the voxel by first exciting magnetization outside the VOI and then dephasing it, while the magnetization inside the VOI is not affected. Notably, SPin ECho full Intensity Acquired Localized spectroscopy (SPECIAL) [31] is a hybrid sequence that uses 1D ISIS localization with the first scan (adiabatic 180° pulse) combined with a SE sequence (90°–180°), as shown in Fig. 2a. It has some of the advantages of STEAM (used with short TE) but it keeps the full signal. However, the add-subtract scheme of the 1D ISIS can cause artifact movements and it is often used with OVS. Note that for all localization approaches the power needed to apply the 90° or 180° pulses needs to be calibrated for each experimental condition.

3.3.2 Suppression of the Water Signal

Suppression of the water signal can be achieved using CHEmical Shift Selective pulses (CHESS) [32]. Values have to be calibrated during each experimental session to obtain a minimum contribution of the water signal to the spectra. This can be achieved by using a sequence with variable-power RF pulses with optimized relaxation delays, like (VAPOR) [33], and selecting the power that minimizes the longitudinal magnetization of water.

3.3.3 Calibrations in ^{13}C Channel

In general, due to the low sensitivity of the ^{13}C signal, calibrations cannot be done in vivo and should be performed previously in vitro in a *phantom* containing a known concentration of ^{13}C labeled molecules. Interestingly, using external bodies during calibration and during the in vivo studies, such as formic acid spheres, is very convenient (*see* Subheading 2).

3.3.4 Decoupling Schemes

Heteronuclear coupling between the X-nucleus and the ^{1}H is relatively large, and decoupling schemes [18] need to be implemented to avoid splitting of the signal in several lines. ^{1}H (or ^{13}C) decoupling is usually done by applying a RF field (B_2) at the Larmor frequency of ^{1}H (or ^{13}C) [13], which can result in increased RF power deposition and cause excessive heating in the tissue. In this sense, it is useful to optimize decoupling power to the minimum. The value should correspond to the minimum power that eliminates most if not all effects of heteronuclear coupling signal.

3.3.5 ^{13}C Editing Block

For ^{1}H-[^{13}C] methods, Adiabatic Full Passage (AFP) pulses in the ^{13}C channel should be also calibrated previously in a *phantom* containing a known concentration of ^{13}C labeled molecules. Optimized power should invert the total ^{1}H-[^{13}C] signal. Figure 2b shows an example of a non-inverted, not-decoupled spectra of labeled acetate (top), and inverted not-decoupled spectra of labeled acetate (middle) after the application of the AFP pulse in the ^{13}C channel. The use of an external reference allows detecting potential variations on the inversion performance of AFP pulses (*see* Subheading 2).

3.4 Tracer Infusion

Infusing a tracer inevitably increases the content of the substance in particular. Because of the non-toxicity of the tracers used and the intrinsic low sensitivity of heteronuclear MRS, the label is normally administered in high quantities, with enrichments ranging between 50 and 100% [34]. Typically, the targeted final IE at steady state is around 70%, and the infusion process is divided in two parts: (1) administration of a bolus of labeled substrate (99% enriched) during a short period of time at an exponential rate and (2) infusion at a constant rate of 70% enriched solution that keeps the IE at steady state during the rest of the experiment. Several factors such as the volume of the glucose bolus infused, rates and time constant of its administration need to be calculated beforehand. The next sections explain in detail these calculations.

3.4.1 Glucose Plasma Levels (Glc_{final})

The amount of ^{13}C glucose in blood at the steady state of IE (Glc_{final}) should be equal to the sum of ^{13}C glucose in blood at initial basal levels (Glc_{basal}), enriched with natural abundance of 1.1%, and the administration of the 99% enriched bolus. This relationship is expressed in Eqs. (4) and (5).

$$Glc_{final} * IR = Glc_{basal} * \frac{1.1}{100} + (Glc_{final} - Glc_{basal}) * \frac{99}{100} \quad (4)$$

With IE = 70%

$$Glc_{final} = Glc_{basal} * \frac{1.1 - 99}{70 - 99} \quad (5)$$

$$\text{if} \quad \frac{1.1-99}{70-99} \cong \frac{1}{(1-70)} \Rightarrow \text{Glc}_{\text{final}} = \frac{1}{(1-\text{IR})}\text{Glc}_{\text{basal}} \tag{6}$$

With IE = 70%

$$\text{Glc}_{\text{final}} = 3.33^{*}\text{Glc}_{\text{basal}} \tag{7}$$

This means that considering Eq. 7 final glucose values can be calculated depending on the targeted IE. If physiological values are to be maintained initial values of blood glucose should be low.

3.4.2 Glucose Bolus Volume

Taking into account that the percentage of extracellular fluid in rodents is around 20% of total body weight [35], and using Eq. 7 to calculate the difference between basal and final glucose concentration, we can estimate that the total glucose bolus administrated in g/kg of animal is 0.0047 * $\text{Glc}_{\text{basal}}$, as expressed in Eq. 8.

$$\begin{aligned}\text{Total glc bolus[g/kg]} &= 0.2^{*}(\text{Glc}_{\text{final}} - \text{Glc}_{\text{basal}}) \\ &= 0.0047^{*}\text{Glc}_{\text{basal}}\end{aligned} \tag{8}$$

As an example, and to proceed with calculations, we will consider a basal glucose level of 90 mg/dL—typical value mice after overnight fasting in mice. We obtain a total bolus of 0.423 g/kg. To transform expression 8 into volume values, we will consider an estimated glucose disposal rate (eGDR) of 33.2 mg/kg/min [36], duration of the bolus of 5 min, and a glucose solution of 200 g/L. The total volume can be calculated as shown in Eq. 9 which corresponds to 2.94 mL/kg of animal in our example.

$$\text{Total glc bolus[mL/kg]} = \left(\text{Total glc bolus[g/kg]} + \frac{\text{eGDR}^{*}5}{1000}\left[\frac{\text{g}}{\text{kg}}\right]\right)^{*}\frac{1000}{200}\left[\frac{\text{mL}}{\text{g}}\right] \tag{9}$$

3.4.3 Rate of Administration of the Bolus

The glucose bolus is habitually administered during 5 min following an exponential decay. To calculate the time constant of the decay (k), we can use the system of equations expressed in Eqs. 10 and 11.

$$V(t=0) = V_0 = 0.45 \cdot \text{Total glc bolus} \tag{10}$$

$$V(t=5) = V_0 \cdot \text{e}^{-\frac{5}{k}} = \text{inf.rate} \tag{11}$$

In Eq. 10 we express the assumption that the 45% of the total bolus is infused in the first minute, while Eq. 11 states the fact that in the last minute of the bolus the amount administered equals the amount calculated with the constant infusion rate of glucose administration (inf. rate) (*see* Subheading 3.4.4 for calculations), both in 1 min.

3.4.4 Infusion Rate

After the administration of the glucose bolus, 70% enriched [1, 6-^{13}C] glucose is infused at a rate equivalent to the eGDR, 33.2 mg/kg/min. If we are using a glucose solution of 200 g/L, this infusion rate can be also expressed as 9.96 mL/kg/h. Ideally, to keep the IE at a steady state, this value might need to be adjusted based depending on concomitantly measured plasma glucose concentrations; if plasma glucose levels decrease infusion rate should be increased by the same percentage, and if plasma glucose levels increase the speed of administration of the glucose solution should be decreased. In rats, these concomitant measurements can be easily done by analyzing the sample extracts of the femoral artery, which are normally performed every 15–30 min. In mice, however, blood extractions are not performed routinely and alternative ways of warranting IE stability are needed. In this respect, there are basically two ways of checking this constancy of IE. The first one consists in taking out the holder from center of the magnet and removing a small drop of blood from the tip of the tail, with the counterpart of having to reposition the animal in the exact same place afterwards. Finally, values can also be checked using the brain glucose and/or lactate FE calculations from MRS measurements.

4 Notes

1. *Glucose measurements.* In experiments with labeled glucose infusions it is critical to measure the blood glucose levels in several time points. Indeed, glucose values are used to calculate the amount of 99% enriched substrate given. Interestingly, it is important to know that the use of some anesthetics, like isoflurane, tend to increase glucose concentration in blood, which is especially true after using high dosages like during induction. Thus, before starting infusion it is useful—particularly in experiments with mice, where blood extractions cannot be performed once the animal is inside the scanner—to measure blood glucose at the following time points: before induction (1), after induction (2) and (3) in the holder before entering the magnet. Ideally, values in (3) should be similar than values in (1), indicating that a sort of stability is reached. If it is the case, and the time between putting the mouse inside the scanner and starting infusion is not too long, the value in (3) can be used to calculate the 99% bolus volume. Otherwise it is recommended to perform a fourth measurement right before starting infusion, removing the mouse form the scanner, with the counterpart of having to position two times the mouse in the magnet. In experiment with bigger animals this can be solved by having a line to extract blood from the femoral artery.

2. *Tail vein vs. femoral vein*. Tail vein cannulations are more fragile than cannulations in femoral vein, but they are mandatory to perform longitudinal studies with measurements at different time points. The protocol for cauterization is similar than for femoral vein, but its smaller size and localization makes it easier for the needle to accidentally come out. This means that animal manipulation has to be done with special care. Also, the smaller size of the vein makes tail vein cannulation more prone to be closed and blocked (partially or completely) the entrance of infusion. To avoid this, two precautions should be taken: keep the tail at warm temperatures while animal preparation and check its circulation by infusing of small amounts of PBS during animal preparation. In fact, once the animal is in the scanner it is always convenient to start infusion only with PBS to keep the line opened. Finally, it is important to take special care of the tail at the end of each MRS session. Sometimes small injuries caused by cannulations can end up with damages in the tail that prevent its usage for the following time points.
3. *Careful positioning of the surface coil*. Being poor sensitivity one of the main issues in heteronuclear MRS, the position of the coil should be optimized to increase SNR in the area of interest. With this aim, it is convenient to perform pilot studies to determine which position enhances mostly the signal in this area. Besides, it is recommended to implement periodically additional tests in phantoms that make sure performance of the coil is not affected.

References

1. Rothman DL, De Feyter HM, de Graaf RA, Mason GF, Behar KL (2011) 13C MRS studies of neuroenergetics and neurotransmitter cycling in humans. NMR Biomed 24 (8):943–957. https://doi.org/10.1002/nbm.1772
2. Zhu XH, Du F, Zhang N, Zhang Y, Lei H, Zhang X, Qiao H, Ugurbil K, Chen W (2009) Advanced in vivo heteronuclear MRS approaches for studying brain bioenergetics driven by mitochondria. Methods Mol Biol 489:317–357. https://doi.org/10.1007/978-1-59745-543-5_15
3. de Graaf RA (2007) Basic principles. In: In vivo NMR spectroscopy. Wiley, pp 1–42. doi: https://doi.org/10.1002/9780470512968.ch1
4. de Graaf RA, Rothman DL, Behar KL (2011) State of the art direct 13C and indirect 1H-[13C] NMR spectroscopy in vivo. A practical guide. NMR Biomed 24(8):958–972. https://doi.org/10.1002/nbm.1761
5. Doddrell DM, Pegg DT, Bendall MR (1982) Distortionless enhancement of NMR signals by polarization transfer. J Magn Reson 48 (2):323–327. https://doi.org/10.1016/0022-2364(82)90286-4
6. Lagemaat MW, van de Bank BL, Sati P, Li SZ, Maas MC, Scheenen TWJ (2016) Repeatability of P-31 MRSI in the human brain at 7T with and without the nuclear Overhauser effect. NMR Biomed 29(3):256–263. https://doi.org/10.1002/nbm.3455
7. Henry PG, Tkac I, Gruetter R (2003) 1H-localized broadband 13C NMR spectroscopy of the rat brain in vivo at 9.4 T. Magn Reson Med 50(4):684–692. https://doi.org/10.1002/mrm.10601
8. Schroeder MA, Atherton HJ, Ball DR, Cole MA, Heather LC, Griffin JL, Clarke K, Radda GK, Tyler DJ (2009) Real-time assessment of Krebs cycle metabolism using hyperpolarized 13C magnetic resonance spectroscopy. FASEB J 23(8):2529–2538. https://doi.org/10.1096/fj.09-129171

9. Ardenkjaer-Larsen JH, Fridlund B, Gram A, Hansson G, Hansson L, Lerche MH, Servin R, Thaning M, Golman K (2003) Increase in signal-to-noise ratio of >10,000 times in liquid-state NMR. Proc Natl Acad Sci U S A 100(18):10158–10163. https://doi.org/10.1073/pnas.1733835100
10. Xin LJ, Lanz B, Lei HX, Gruetter R (2015) Assessment of metabolic fluxes in the mouse brain in vivo using H-1-[C-13] NMR spectroscopy at 14.1 Tesla. J Cerebr Blood F Met 35 (5):759–765. https://doi.org/10.1038/jcbfm.2014.251
11. Lizarbe B, Cherix A, Xin L, Lei H, Gruetter R (2016) In vivo detection of hypothalamic glucose metabolism in HFD and regular fed mice. Proceedings of the 24th Annual Meeting ISMRM, Singapore, p.110.
12. Vuister GW, Ruizcabello J, Vanzijl PCM (1992) Gradient-enhanced multiple-quantum filter (ge-MQF)—a simple way to obtain single-scan phase-sensitive HMQC spectra. J Magn Reson 100(1):215–220. https://doi.org/10.1016/0022-2364(92)90381-G
13. Pfeuffer J, Tkac I, Choi IY, Merkle H, Ugurbil K, Garwood M, Gruetter R (1999) Localized in vivo 1H NMR detection of neurotransmitter labeling in rat brain during infusion of [1-13C] D-glucose. Magn Reson Med 41(6):1077–1083
14. Xin LJ, Mlynarik V, Lanz B, Frenke H, Gruetter R (2010) (1)H-[(13)C] NMR spectroscopy of the rat brain during infusion of [2-(13)C] acetate at 14.1 T. Magn Reson Med 64 (2):334–340. https://doi.org/10.1002/mrm.22359
15. Duarte JM, Lei H, Mlynarik V, Gruetter R (2012) The neurochemical profile quantified by in vivo 1H NMR spectroscopy. NeuroImage 61(2):342–362. https://doi.org/10.1016/j.neuroimage.2011.12.038
16. Duarte JM, Gruetter R (2013) Glutamatergic and GABAergic energy metabolism measured in the rat brain by (13) C NMR spectroscopy at 14.1 T. J Neurochem 126(5):579–590. https://doi.org/10.1111/jnc.12333
17. Cudalbu C, Lanz B, Duarte JM, Morgenthaler FD, Pilloud Y, Mlynarik V, Gruetter R (2012) Cerebral glutamine metabolism under hyperammonemia determined in vivo by localized (1)H and (15)N NMR spectroscopy. J Cerebr Blood F Met 32(4):696–708. https://doi.org/10.1038/jcbfm.2011.173
18. Gruetter R, Adriany G, Choi IY, Henry PG, Lei H, Oz G (2003) Localized in vivo 13C NMR spectroscopy of the brain. NMR Biomed 16(6-7):313–338. https://doi.org/10.1002/nbm.841
19. Adriany G, Gruetter R (1997) A half-volume coil for efficient proton decoupling in humans at 4 tesla. J Magn Reson 125(1):178–184. https://doi.org/10.1006/jmre.1997.1113
20. Lizarbe B, Cherix A, Lei H, Gruetter R (2015) In vivo 13C spectroscopy of the mouse hypothalamus. In: ESMRMB, Edinburgh
21. Waniewski RA, Martin DL (1998) Preferential utilization of acetate by astrocytes is attributable to transport. J Neurosci 18 (14):5225–5233
22. Duarte JM, Girault FM, Gruetter R (2015) Brain energy metabolism measured by (13)C magnetic resonance spectroscopy in vivo upon infusion of [3-(13)C]lactate. J Neurosci Res 93 (7):1009–1018. https://doi.org/10.1002/jnr.23531
23. Henry PG, Adriany G, Deelchand D, Gruetter R, Marjanska M, Oz G, Seaquist ER, Shestov A, Ugurbil K (2006) In vivo 13C NMR spectroscopy and metabolic modeling in the brain: a practical perspective. Magn Reson Imaging 24(4):527–539. https://doi.org/10.1016/j.mri.2006.01.003
24. Sibson NR, Mason GF, Shen J, Cline GW, Herskovits AZ, Wall JE, Behar KL, Rothman DL, Shulman RG (2001) In vivo (13)C NMR measurement of neurotransmitter glutamate cycling, anaplerosis and TCA cycle flux in rat brain during. J Neurochem 76(4):975–989
25. Gargiulo S, Greco A, Gramanzini M, Esposito S, Affuso A, Brunetti A, Vesce G (2012) Mice anesthesia, analgesia, and care, Part I: anesthetic considerations in preclinical research. ILAR J 53(1):E55–E69. https://doi.org/10.1093/ilar.53.1.55
26. Tkac I, Henry PG, Andersen P, Keene CD, Low WC, Gruetter R (2004) Highly resolved in vivo 1H NMR spectroscopy of the mouse brain at 9.4 T. Magn Reson Med 52 (3):478–484. https://doi.org/10.1002/mrm.20184
27. Bottomley PA (1987) Spatial localization in NMR spectroscopy in vivo. Ann N Y Acad Sci 508:333–348
28. Frahm J, Bruhn H, Gyngell ML, Merboldt KD, Hanicke W, Sauter R (1989) Localized high-resolution proton NMR spectroscopy using stimulated echoes: initial applications to human brain in vivo. Magn Reson Med 9 (1):79–93
29. Tkac I, Starcuk Z, Choi IY, Gruetter R (1999) In vivo 1H NMR spectroscopy of rat brain at 1 ms echo time. Magn Reson Med 41 (4):649–656
30. Ordidge RJ, Connelly A, Lohman JAB (1986) Image-selected invivo spectroscopy (Isis)—a

new technique for spatially selective NMR-spectroscopy. J Magn Reson 66 (2):283–294. https://doi.org/10.1016/0022-2364(86)90031-4

31. Mlynarik V, Gambarota G, Frenkel H, Gruetter R (2006) Localized short-echo-time proton MR spectroscopy with full signal-intensity acquisition. Magn Reson Med 56 (5):965–970. https://doi.org/10.1002/mrm.21043
32. Haase A, Frahm J, Hanicke W, Matthaei D (1985) 1H NMR chemical shift selective (CHESS) imaging. Phys Med Biol 30 (4):341–344
33. Tkac I, Gruetter R (2005) Methodology of H NMR spectroscopy of the human brain at very high magnetic fields. Appl Magn Reson 29 (1):139–157. https://doi.org/10.1007/BF03166960
34. Gruetter R (2002) In vivo 13C NMR studies of compartmentalized cerebral carbohydrate metabolism. Neurochem Int 41(2-3):143–154
35. Chapman ME, Hu L, Plato CF, Kohan DE (2010) Bioimpedance spectroscopy for the estimation of body fluid volumes in mice. Am J Physiol Ren Physiol 299(1):F280–F283. https://doi.org/10.1152/ajprenal.00113.2010
36. Jucker BM, Schaeffer TR, Haimbach RE, McIntosh TS, Chun D, Mayer M, Ohlstein DH, Davis HM, Smith SA, Cobitz AR, Sarkar SK (2002) Normalization of skeletal muscle glycogen synthesis and glycolysis in rosiglitazone-treated Zucker fatty rats: an in vivo nuclear magnetic resonance study. Diabetes 51(7):2066–2073